Efficient Prediction of Isotropic Hyperfine Coupling in Radicals Containing Phosphorus. A Systematic Comparison of UHF, PUHF, and UMP2 Spin Densities

2 AUTHORS, INCLUDING:

Christopher J Cramer
University of Minnesota Twin Cities

532 PUBLICATIONS **23,456** CITATIONS

Efficient Prediction of Isotropic Hyperfine Coupling in Radicals Containing Phosphorus. A Systematic Comparison of UHF, PUHF, and UMP2 Spin Densities

Christopher J. Cramer* and Myong H. Lim

Department of Chemistry and Supercomputer Institute, University of Minnesota, 207 Pleasant St. SE, Minneapolis, Minnesota 55455-0431

Received: November 12, 1993; In Final Form: February 11, 1994[⊕]

Isotropic hyperfine couplings have been calculated and compared to experiment for 25 radicals containing phosphorus using the 6-311G** basis set. At HF/6-31G** optimized geometries, Fermi contact integrals derived from UMP2 spin-density matrices give the best correlation with experiment (20 data points for ^{31}P, 8 data points for ^{19}F, 7 data points for ^{35}Cl, and 5 data points for ^{1}H hyperfine couplings, rms error of 22.9 G with the data spanning a range of about 1650 G); PUHF spin-density matrices are somewhat less useful (rms error of 33.6 G), and calculation at the UHF level gives poor results (rms error of 45.6 G). Hyperfine couplings calculated at the UMP2 level may be scaled by 102% to bring them into closer agreement with experiment. Even though geometric changes on going to the MP2 level may be sizable, better correlation with experiment is obtained when HF/6-31G** optimized geometries are used instead of MP2/6-31G** optimized geometries (rms error of 36.1 G). Including diffuse functions in the calculation of the hyperfine couplings for anionic radicals has in general only marginal effect. Statistical trends within specific subsets of the data are also discussed.

1. Introduction

Phosphoranyl radicals, which are tetracoordinate open-shell species analogous to phosphoranes, are stereochemically fascinating.[1–5] A typical mode of generation involves addition of a radical to a phosphine, resulting in a trigonal-bipyramidal phosphorus species, with the unpaired electron occupying one position of the trigonal bipyramid (TBP).[1] Addition and elimination to and from TBPs are typically thought to occur apically; kinetic analysis of such processes in tetraalkoxyphosphoranyl radicals appears to indicate that stereopermutation of axial and equatorial ligands is very rapid.[1,6–10] This is consistent with the relatively low barriers which have been calculated for stereopermutation in hydroxylated phosphoranyl radicals.[11–13]

Structural characterization of phosphoranyl radicals has largely been accomplished using electron spin resonance (ESR) spectroscopy.[1,6–10,14–33] Based on this method, the vast majority of phosphoranyl radicals appear to be TBP in overall structure, with the unpaired electron localized equatorially, so-called TBP$_e$. Several examples also exist of phosphoranyl radicals which are slightly distorted from an essentially tetrahedral geometry, so-called DT; in these radicals the unpaired electron is assigned to a P–X antibonding orbital.[7,14–18,25–29,33] Another possibility is for the unpaired electron to be localized axially in the TBP, i.e., TBP$_a$; however, such assignments have been rare[22,23] and hotly debated.[5] Theoretical calculations indicate the unpaired electron to be strongly apico*phobic*,[2–5,11–13,16,17,20,21,24,27,34–39] although it has recently been illustrated that other electronic effects can overwhelm this apicophobicity and render certain TBP$_a$ structures stable.[12] Finally, other structures such as a square-planar arrangement with the unpaired electron in the p orbital orthogonal to the plane, or square-pyramidal structures where the unpaired electron again acts as a fifth substituent, have never been observed experimentally; theory invariably finds such structures to be saddle points on the molecular potential energy hypersurface.[2–5,11–13,35–37]

Of course, structural assignment based on spectral data requires spectral interpretation, which is not always entirely straightforward. The evaluation of competing structural proposals may be significantly facilitated by recourse to theoretical methods, e.g., predicted ESR hyperfine couplings.

2. ESR Prediction

The calculation of ESR hyperfine couplings (hfs) has received a great deal of attention.[16,34,39–52] In general, the *isotropic* hyperfine coupling to nucleus X, a_X, is calculated from

$$a_X = (8\pi/3)gg_X\beta\beta_X\rho(X) \qquad (1)$$

where g is the electronic g factor, typically set to 2.0, β is the Bohr magneton, g_X and β_X are the analogous values for nucleus X, and $\rho(X)$ is the Fermi contact integral. The latter term corresponds to the unpaired spin density at the nuclear position. For calculational methodologies which expand the spin density in terms of electronic occupation over a finite basis set, the Fermi contact integral is evaluated from

$$\rho(X) = \sum_{\mu\nu}P_{\mu\nu}^{\alpha-\beta}\phi_\mu(R_X)\,\phi_\nu(R_X) \qquad (2)$$

where $P^{\alpha-\beta}$ is the one-electron spin-density matrix, the summation runs over all basis functions ϕ, and the evaluation of the overlap between elements μ and ν is only at the nuclear position, R_X. The one-electron spin-density matrix is available for a wide variety of methodologies, including semiempirical approaches[53–55] like the CNDO, INDO, and NDDO models,[38,46,49,56] unrestricted (UHF) and restricted (ROHF) Hartree–Fock[57–59] approaches, post-Hartree–Fock treatments[57–59] using many-body perturbation theory (MP2)[34,35,43,50,60,61] and configuration interaction (CI),[41,42,44,45,47,60,62–72] and more recent explorations[40] including density functional methods.[73–75] Another alternative is pseudoorbital theory.[48,76] Finally, when one-electron density matrices are not readily calculable, the finite field methodology allows evaluation of the Fermi contact integral by an appropriate perturbation of the quantum mechanical Hamiltonian.[50,60,69,70]

The key to ensuring accurate predictions from eq 1, of course, is that the density matrix employed is derived from an accurate wave function. In particular, localization of excess spin must be treated accurately. Restricted open-shell methods, which handle doubly-filled and partially-filled orbitals in formally separate ways, can be quite effective in delivering good "first-order" wave functions. However, they do not permit doubly-filled orbitals to be spin-polarized (therefore failing to assign any unpaired spin

density at the nuclei in the planar methyl radical, for instance). ROHF methods also usually deliver a single-determinantal wave function, and it remains technically challenging to include the effects of correlation into these wave functions.

Unrestricted methods, on the other hand, implicitly evaluate α and β exchange interactions separately and thus are able to account for both spin polarization and some small amount of configurational mixing. As a result, however, wave functions derived from unrestricted methods are generally *not* eigenfunctions of the operator S^2 and as such are contaminated by higher spin states. The trick in using unrestricted methods lies in eliminating the undesired spin "contamination" while maintaining the useful spin "polarization".

This is all made somewhat more difficult insofar as it is at the nuclear positions that one must accurately predict excess spin density in order to calculate the isotropic hfs values. Although core s orbitals on a given atom will in general be only very weakly polarized by unpaired spin density in a valence orbital, the amplitude at the nucleus of such orbitals is very large, so it is not safe to ignore such effects in the core.[77-79] Moreover, atomic s orbitals are characterized by a cusp at the nucleus; such a condition is accurately modeled by basis sets of Slater type orbitals[48,76] but can only be approximated with the more computationally efficient Gaussian type orbitals.

In principle, one can solve all of these problems by doing variational multireference configuration interaction calculations with large, flexible, uncontracted basis sets, and this has been accomplished for a number of small molecules.[45,47,66,67,72] Obviously, however, such an approach is not currently feasible for systems comprising more than a very few heavy atoms. Instead, single-reference wave functions are more tractable, as are correlation treatments along the lines of many-body perturbation theory. Of these, the second-order theory (MP2) is the most efficient.[57-59]

A virtue of post-Hartree–Fock treatments of unrestricted wave functions is that they tend to have considerably reduced spin contamination.[57-59] However, this same effect can be accomplished by the use of a simple projection operator formalism (PUHF),[80] which takes essentially no time beyond the UHF calculation itself. PUHF densities have in many instances proven efficacious for hfs prediction.[16,25,35,39,42,52,81-83] Of course, the PUHF approach does *not* take account of the correlated motions of the electrons, except to the extent that the UHF wave function includes some configurational mixing by virtue of separately treating the α and β molecular orbitals.[57-59]

We are primarily interested in comparing those methodologies which may be most conveniently applied to relatively large systems at an ab initio level. Given our interest in phosphoranyl radicals and the relative wealth of data on open-shell systems containing phosphorus, we have selected a set of 25 radicals, including cations, neutral molecules, and anions, from which a total of 40 experimental hfs values are available for ^{31}P, ^{19}F, ^{35}Cl and ^{1}H nuclei.[17,19,32,36,84-100] We compare experimental values with those calculated at the UHF, PUHF, and UMP2 levels with the 6-311G** basis set.[101-103] We have found this basis to be a good compromise between speed and accuracy.[34,43] We also examine the effects of geometry optimization at various levels and of having diffuse functions added to the basis set for anions. Section 3 describes the calculational details, section 4 provides the calculated geometries and hyperfine couplings, and section 5 discusses the correlation with experiment observed for various theoretical levels.

Finally, we should explicitly note that we are ignoring any effects of vibrational averaging on hfs values. This phenomenon can be quite important in open-shell molecules which have low-frequency modes over which the hyperfine coupling is nonuniform; i.e., the expectation value for hfs differs from that calculated for the equilibrium structure.[41,60-62,69,70,82,104-106] However, the majority of the radicals studied here do not appear to be especially sensitive in this regard, nor is it generally feasible to correct for

vibrational motion in larger systems with complicated normal modes and little symmetry.

3. Computation Methods

Molecular geometries were fully optimized at the UHF and UMP2 levels of theory[58] employing the 6-31G** basis set.[107] Core orbitals were included in the excitation windows for the MP2 calculations. The nature of all stationary points was verified by analytic calculation of harmonic frequencies at the Hartree–Fock level.[58] In a number of instances where the central phosphorus atom bore two oxygen or two sulfur substituents which could be regarded as formally doubly bonded, either an imaginary frequency or one frequency with an unusually large intensity (e.g., 20 000 km/mol) of the same symmetry as the overall electronic wave function was obtained at the Hartree–Fock level. These arise from artifactual HF doublet-instability.[108-110] Doublet instability was verified by the observation of significant energy lowering for identical structures when the electronic wave function was permitted to have broken symmetry relative to the molecular point group (either C_{2v} or C_s). At correlated levels, negative force constants are not observed, although the nature of the normal mode may remain unrealistically far from harmonic in the absence of reasonably sophisticated treatments. Doublet instability causes both HF vibrational frequencies and hyperfine couplings to be quite suspect. However, as illustrated below, the latter quantities appear to be predicted fairly accurately upon going to the MP2 level. All electronic wave functions were checked for stability, regardless of whether unusual frequencies were obtained from the vibrational analysis.

Calculation of hfs values was accomplished using eqs 1 and 2 above, using the 6-311G** basis set with one-electron spin-density matrix elements taken from UHF, PUHF, and UMP2 wave functions. For anions, the 6-311+G* basis set was also employed. (Note that none of the anions considered here contain hydrogen atoms, so no functions have been removed relative to 6-311G**.[58]) The calculations were carried out for both UHF and UMP2 optimized geometries.

Linear regression of predicted hyperfine couplings against experimental values mandated the selection of a single experimental result when more than one was available. As a rule, we tried to avoid experimental results where a large potential for error was noted. In addition, we tried to choose the experimental conditions which could most be regarded as "gas-phase-like", although there are a few instances where large variations, which appear to depend on matrix effects, are observed. These are detailed in the results section. In general, ^{35}Cl hyperfine splittings were reported with larger error bars than for ^{31}P, ^{19}F, or ^{1}H.

All calculations employed the Gaussian92 suite of electronic structure programs.[111]

4. Results

Figure 1 presents the critical geometrical details for the 25 molecules in this study at both the UHF and UMP2 levels. A complete specification of geometries and absolute energies is provided as supplementary material. Table 1 lists the HF harmonic vibrational frequencies and intensities for each ground electronic state; imaginary frequencies arise for selected cases as a result of the Hartree–Fock doublet instability[108-110] present in **8, 12, 15,** and **22–25.** Table 2 presents the experimental and calculated hyperfine couplings (using the 6-311G** basis set). Table 3 includes the calculated hfs values for the anions when diffuse functions are added to the basis set. Table 4 presents the error analysis and regression statistics for the various combinations of geometry, basis set, and theoretical level, for specific subsections of the data, and for the entire data set. The linear regression for the full data set using UMP2 derived Fermi contact integrals at HF geometries is illustrated in Figure 2.

$H_2POH^+(^2A)$. This cation has been studied previously by Aagaard at the UHF and ROHF levels with the 6-31G* basis set,[16] and our predicted geometry using the 6-31G** basis is
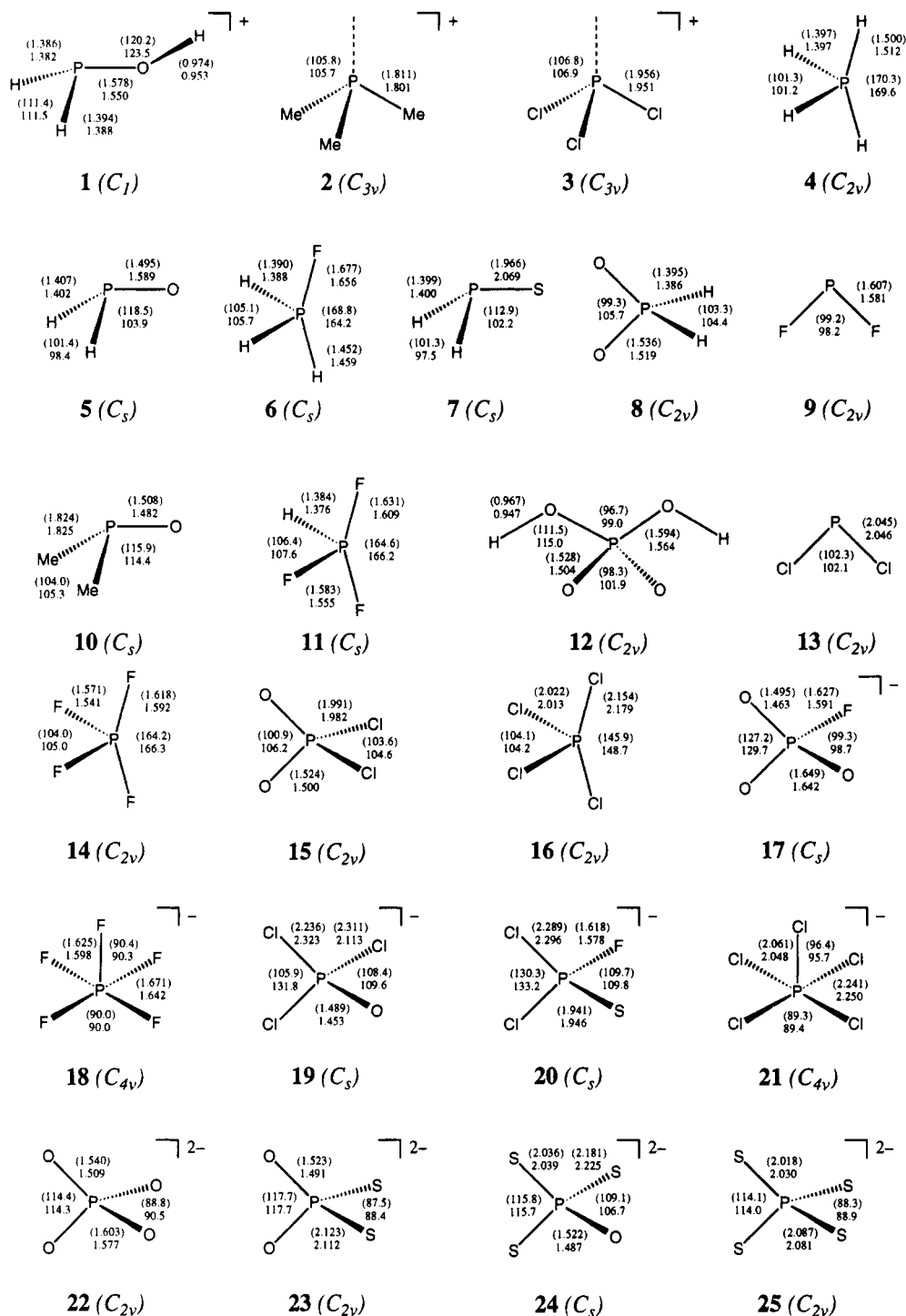
$1\ (C_1)$ $2\ (C_{3v})$ $3\ (C_{3v})$ $4\ (C_{2v})$

$5\ (C_s)$ $6\ (C_s)$ $7\ (C_s)$ $8\ (C_{2v})$ $9\ (C_{2v})$

$10\ (C_s)$ $11\ (C_s)$ $12\ (C_{2v})$ $13\ (C_{2v})$

$14\ (C_{2v})$ $15\ (C_{2v})$ $16\ (C_{2v})$ $17\ (C_s)$

$18\ (C_{4v})$ $19\ (C_s)$ $20\ (C_s)$ $21\ (C_{4v})$

$22\ (C_{2v})$ $23\ (C_{2v})$ $24\ (C_s)$ $25\ (C_{2v})$

Figure 1. Selected geometrical data and symmetry information for **1–25**. Bond lengths are in angstroms, bond angles in degrees.

essentially the same. The isotropic hfs values indicate the unpaired electron to reside primarily on phosphorus; with the smaller, less flexible 6-31G* basis Aagaard predicted a similar ^{31}P coupling of 495 G at the UHF level. The conjugate base of this molecule, H$_2$PO (vide infra), shows extreme sensitivity to level of theory as regards localization of the unpaired electron. Protonation, however, significantly decreases any tendency for the unpaired electron to localize on oxygen. Janssen et al.[27,29] have argued that this effect is overemphasized in gas-phase calculations based on experimental studies of anionic, neutral, and cationic thiophosphoranyl radicals. No data are available for the present case.

Me$_3$P$^+$($^2A_1$). Begum and Symons[87] reported an experimental observation of **2** in H$_2$SO$_4$ solution with an isotropic ^{31}P hfs of 393.3 G. Janssen et al.[29] observed this radical in an X-irradiated CFCl$_3$ matrix at 77 K and obtained a similar ^{31}P coupling (388.9

G) as well as a 12.1 G coupling to nine equivalent ^{1}H nuclei. The MP2 predicted ^{31}P hfs values are in excellent accord with these measurements. The equivalence of the protons implies rapid rotation of the methyl groups; by averaging the ^{1}H couplings for the theoretical equilibrium structure, we obtain a rough estimate of about 11 G for the rotationally averaged MP2 hyperfine splitting, again in good agreement with the experiment. Prior theoretical studies of this molecule have not appeared.

PCl$_3^+$($^2A_1$). Aagaard et al.[16,17] have studied this molecule in various X-irradiated halocarbon matrices at 98 K. In matrices containing fluorine, they observe a ^{31}P hfs of 833.5 G and a ^{35}Cl hfs of 23.3 G. Our theoretical values are not in particularly good agreement with either observation. Since we calculate the inversion barrier for this molecule to be on the order of 40 kcal/mol at our highest level, this does not appear to be a problem of ignoring vibrational motion. It appears instead that some of the

TABLE 1: Hartree–Fock Vibrational Frequencies for Radicals 1–25[a,b]

radical	ground electronic state	frequency (symmetry, intensity)
1	^2A	367 (A, 200); 859 (A, 100); 945 (A, 50); 997 (A, 200); 1120 (A, 30); 1170 (A, 40); 2684 (A, 2); 2754 (A, 5); 4066 (A, 500)
2	$^2A_1$	139 (A_2, 0); 161 (E, 0); 248 (E, 2) 253 (A_1, 1) 660 (A_1, 0) 805 (E, 3); 898 (A_2, 0); 907 (E, 0); 1073 (A_1, 30); 1081 (E, 50); 1471 (E, 10); 1496 (A_1, 10); 1548 (A_2, 0); 1559 (E, 2); 1566 (E, 20); 1581 (A_1, 50); 3191 (E, 4); 3193 (A_1, 1); 3284 (E, 0); 3286 (A_1, 7); 3309 (A_2, 0); 3311 (E, 5)
3	$^2A_1$	213 (E, 5); 289 (A_1, 10); 537 (A_1, 10); 702 (E, 200)
4	$^2A_1$	930 (B_1, 40); 1024 (A_1, 40); 1091 (A_1, 2); 1159 (B_2, 500); 1310 (A_2, 0); 1426 (B_2, 300); 1838 (A_1, 20); 2611 (A_1, 40); 2622 (B_1, 90)
5	$^2A'$	603 (A', 30); 934 (A'', 10); 1001 (A', 40); 1252 (A', 40); 2578 (A', 80); 2585 (A'', 4)
6	$^2A'$	662 (A'', 20); 715 (A', 200); 807 (A', 50); 1062 (A', 40); 1301 (A', 100); 1308 (A'', 20); 2092 (A', 300); 2675 (A', 30); 2690 (A'', 90)
7	$^2A'$	500 (A', 0); 802 (A', 10); 861 (A'', 5); 1241 (A', 50); 2591 (A', 70); 2595 (A'', 90)
8	$^2B_2{}^c$	341 (A_1, 1); 902 (B_1, 1); 925 (A_2, 0); 1131 (A_1, 7); 1169 (B_2, 1); 1289 (A_1, 100); 1990 (B_2, 9000); 2696 (B_1, 100); 2703 (A_1, 90)
9	$^2B_1$	384 (A_1, 10); 931 (B_2, 200); 940 (A_1, 100)
10	$^2A'$	166 (A'', 0); 190 (A', 1); 267 (A', 0); 331 (A'', 20); 339 (A', 10); 704 (A', 5); 784 (A'', 30); 885 (A'', 1); 955 (A'', 40); 973 (A', 10); 1036 (A', 10); 1252 (A', 90); 1460 (A'', 10); 1473 (A', 10); 1576 (A'', 6); 1582 (A'', 1); 1585 (A', 4); 1597 (A', 20); 3187 (A'', 5); 3190 (A', 6); 3268 (A'', 10); 3292 (A'', 4); 3293 (A', 8)
11	$^2A'$	325 (A', 20); 350 (A', 30); 456 (A'', 10); 700 (A', 8); 945 (A'', 400); 956 (A', 60); 1018 (A', 200); 1278 (A'', 40); 2771 (A', 60)
12	$^2B_1{}^c$	119 (A_2, 0); 329 (B_1, 200); 359 (A_1, 20); 389 (A_2, 0); 456 (A_1, 4); 469 (B_2, 100); 572 (B_1, 300); 937 (A_1, 10); 1007 (B_2, 300); 1097 (A_1, 200); 1142 (B_2, 50); 1275 (A_1, 400); 2443 (B_1, 20000); 4165 (B_2, 400); 4167 (A_1, 9)
13	$^2B_1$	227 (A_1, 3); 552 (B_2, 200); 558 (A_1, 70)
14	$^2A_1$	247 (A_1, 0); 302 (B_1, 10); 417 (A_2, 0); 509 (B_2, 20); 522 (A_1, 60); 714 (A_1, 10); 976 (B_2, 500); 996 (A_1, 200); 1047 (B_1, 200)
15	$^2B_2{}^c$	228 (A_1, 0); 256 (A_1, 0); 357 (A_1, 30); 383 (B_2, 60); 387 (B_1, 30); 575 (A_1, 60); 687 (B_1, 400); 1191 (A_1, 200); 2095 (B_2, 9000)
16	$^2A_1$	114 (B_2, 100); 127 (A_1, 2); 154 (B_1, 4); 190 (A_2, 0); 253 (A_1, 5); 305 (B_2, 200); 306 (A_1, 8); 570 (A_1, 100); 611 (B_1, 200)
17	$^2A''$	301 (A'', 4); 350 (A', 1); 484 (A'', 40); 538 (A', 60); 544 (A', 60); 852 (A', 90); 895 (A', 300); 1233 (A', 200); 1466 (A'', 400)
18	$^2A_1$	246 (B_2, 0); 340 (E, 0); 442 (B_1, 0); 517 (E, 8); 567 (A_1, 50); 589 (B_2, 0); 651 (A_1, 10); 880 (E, 500); 910 (A_1, 10)
19	$^2A'$	84 (A', 1); 99 (A'', 90); 156 (A', 5); 187 (A'', 60); 243 (A', 10); 328 (A', 20); 426 (A'', 400); 488 (A', 300); 1367 (A', 300)
20	$^2A'$	93 (A'', 100); 104 (A', 3); 191 (A', 7); 233 (A'', 100); 251 (A', 20); 346 (A', 30); 384 (A'', 300); 663 (A', 200); 916 (A', 200)
21	$^2A_1$	83 (B_2, 0); 156 (E, 90); 200 (E, 100); 222 (B_1, 0); 231 (B_2, 0); 240 (A_1, 10); 288 (A_1, 5); 329 (E, 400); 553 (A_1, 100)
22	$^2B_2{}^c$	369 (A_2, 0); 407 (A_1, 1); 563 (B_1, 50); 566 (A_1, 60); 606 (B_2, 100); 964 (A_1, 30); 1195 (A_1, 400); 1254 (B_1, 400); 2093 (B_2, 20000)
23	$^2B_2{}^c$	965i (B_2, 24000); 217 (A_1, 0); 253 (A_2, 0); 377 (B_1, 10); 386 (B_2, 5); 435 (A_1, 0); 603 (A_1, 200); 1145 (A_1, 400); 1327 (B_1, 300)
24	$^2A''{}^c$	116i (A'', 0); 186 (A', 0); 274 (A', 8); 318 (A', 20); 385 (A'', 10); 444 (A', 100); 532 (A', 200); 656 (A'', 300); 1249 (A', 300)
25	$^2B_2{}^c$	753i (B_2, 24000); 171 (A_2, 0); 192 (A_1, 0); 263 (A_1, 7); 264 (B_1, 5); 313 (B_2, 200); 441 (A_1, 0); 638 (A_1, 200); 642 (B_1, 200)

[a] Frequencies in cm^{-1}, intensities in km/mol. [b] Calculated at the HF/6-31G** level. [c] Wave function exhibits Hartree–Fock doublet instability.

discrepancy may arise because of interaction with the matrix in the experimental situation. This is not entirely speculative, since switching the matrix to CH_2Cl_2 delivers a ^{31}P hfs of 959.5 G, a fairly large change from the other matrices. Nevertheless, we include the former data in the regression analysis. Aagaard et al. have optimized the geometry of $PCl_3{}^+$ at the ROHF/ 3-21G$^{(*)}$ level, obtaining a P–Cl bond length of 2.039 Å, an umbrella angle of 117.4°, and calculated ^{31}P and ^{35}Cl hfs of 522.0 and 2.9 G, respectively. The small size of the basis set accounts for the fairly large discrepancies both with our calculations and with experiment.

$PH_4(^2A_1)$. This prototypical phosphoranyl radical has been studied extensively, both experimentally[91] and theoretically.[2–5,34] As we have discussed 4 in more detail elsewhere,[34] we restrict ourselves here to recognizing that the structure of this radical is a distorted trigonal bipyramid with the unpaired electron occupying an equatorial position. There is uniform agreement among theoretical studies that the TBP$_e$ geometry localizes spin primarily on the axial protons and on phosphorus. The alternative TBP$_a$ structure, which places the unpaired electron in an axial position and is not a mimimum, localizes spin primarily on the equatorial protons. These generalizations are, however, subject to some change when other substituents replace the protons.[11,13] The present calculations predict hyperfine splittings in good agreement with experiment.

$H_2PO(^2A')$. The P–O bond length in 5 proves to be exquisitely sensitive to level of theory, shortening by a full 0.1 Å on going from UHF to UMP2 with the 6-31G** basis set.[112] Aagaard et al.[16] have discussed this in terms of a competition between resonance contributors representing an oxygen-centered radical (long bond) and a zwitterionic phosphorus-centered radical (short bond). They demonstrated that there are two nearly degenerate a' orbitals which may contain the unpaired electron by finding separate ROHF minima for both resonance structures. Such a finding is an artifact of the separate treatment of doubly-occupied and singly-occupied orbitals at the latter level of theory. This subtlety appears to depend closely on the proton substitution at phosphorus, since the methyl groups in 10 make the analogous P–O bond length there much less sensitive to level of theory.

Experimental measurements for this radical have not appeared; however, a number of alkyl- and aryl-substituted analogs have been observed to have ^{31}P hyperfine couplings in the 330–390-G range.[16] It is not clear whether deviations of the MP2 hfs values from this range legitimately arise because of the unique nature of the proton substituents, because of dynamic effects, or because they are artifacts of a clearly unconverged P–O bond length. Higher-level studies will be required to resolve this issue.

$H_3PF(^2A')$. Radical 6 is another member of the fluorophosphoranyl series which has seen extensive experimental[19,91,92,97] and theoretical[3,19,34] study. We have discussed the fluorophosphoranyl series in more detail elsewhere[34] and point out here only the excellent agreement between experimental and MP2-derived hfs values for all four distinct nuclei.

$H_2PS(^2A')$. Radical 7, like its oxygen analog 5, has a bond length between the heavy atoms which is extremely sensitive to level of theory. This is in contrast to tetrasubstituted phosphoranyl sulfides.[16,17,24,25,27,29,35,37] As with 5, there are no available experimental data for 7. Alkyl- and aryl-substituted analogs[25] have ^{31}P couplings in a range from 295 to 370 G. It is again not clear to what extent the deviation of the MP2/MP2 result from this range can be considered to be trustworthy. Although the predicted hfs values are provided for consistency, it appears that very high levels of theory would probably be required to adequately converge the calculated values with respect to basis set, correlation treatment, and potentially P–X bond vibrational stretching and/ or fluctional motion.[16,112]

$H_2PO_2(^2B_2)$. We have discussed 8 in the context of the hydrogen substitution reaction at phosphorus in HPO_2[109] and the cheletropic reaction of H_2 and PO_2.[113] Those cases involved the $^2B_1$ electronic state, which is the ground state at the MP2/6-31G** level of theory but lies about 6 kcal/mol above the $^2B_2$ state at the QCISD-(T)/6-31G**//MP2/6-31G** level. Both of these electronic states exhibit Hartree–Fock doublet instability, as judged by the decrease in electronic energy upon allowing the molecular wave function to break symmetry. Unlike the $^2B_1$ state,[109] the $^2B_2$ state does not give an anomalous imaginary frequency; instead, an unusually intense absorption at 1990 cm^{-1} is predicted. One or the other of these two phenomena appears to be present in each

TABLE 2: Calculated and Experimental Hyperfine Couplings for Radicals 1–25[a]

			Isotropic hyperfine coupling, G							
			UHF/6-31G** geometry			MP2/6-31G** geometry				
radical	HF $\langle S^2 \rangle$	nucleus	UHF	PUHF	UMP2	UHF	PUHF	UMP2	expt[b]	ref[c]
1	0.7562	^{31}P	575.1	519.6	507.2	583.6	531.1	509.7		
		^{17}O	−12.8	−5.0	−6.4	−12.6	−4.9	−6.7		
		^{1}H(P)	18.6	19.7	20.2	19.2	20.0	21.1		
		^{1}H(P)	31.1	28.0	33.2	33.2	29.1	35.5		
		^{1}H(O)	−6.5	−2.0	−4.6	−6.8	−2.1	−4.8		
2	0.7556	^{31}P	461.1	372.2	402.3	459.6	371.9	394.7	393.3	87
		^{13}C	0.5	3.5	1.4	0.6	3.7	1.6		
		^{1}H$_{anti}$	27.4	18.2	28.5	28.0	18.6	28.9		
		^{1}H$_{syn}$	1.4	1.1	1.5	1.5	1.2	1.5		
3	0.7617	^{31}P	804.8	767.7	767.1	804.1	768.3	763.3	833.5	17
		^{35}Cl	4.9	4.2	7.2	4.7	4.1	6.8	23.3	
4	0.7758	^{31}P	492.9	506.6	512.0	481.2	497.0	499.9	519.3	91
		^{1}H$_{ax}$	192.4	149.7	179.1	191.0	148.9	179.1	198.7	
		^{1}H$_{eq}$	−17.7	−4.1	−9.2	−17.3	−3.8	−8.6	−6.0	
5	0.7757	^{31}P	87.7	93.7	206.8	345.2	323.7	456.1		
		^{17}O	−31.2	−10.8	−14.4	−30.5	−11.6	−0.6		
		^{1}H	29.4	17.2	37.3	25.8	21.4	28.9		
6	0.7640	^{31}P	784.3	728.9	720.1	805.6	747.9	740.4	721.3	91
		^{19}F	370.7	282.0	309.2	382.6	291.0	317.4	347.2	
		^{1}H$_{ax}$	125.1	97.1	112.6	122.0	94.8	110.8	130.1	
		^{1}H$_{eq}$	−24.7	−7.8	−15.4	−24.7	−7.8	−15.0	−12.6	
7	0.7722	^{31}P	70.4	62.9	112.8	181.8	153.6	249.2		
		^{33}S	11.6	4.4	8.4	12.5	4.7	5.7		
		^{1}H	18.1	10.4	18.4	19.5	13.2	18.7		
8	0.8131	^{31}P	−173.2	−55.2	−22.7	−162.1	−51.9	−22.2		
		^{17}O	−11.3	−4.8	−3.6	−14.7	−6.5	−4.9		
		^{1}H	−3.6	−1.2	−4.8	−3.9	−1.3	−4.6		
9	0.7696	^{31}P	217.2	77.8	90.1	221.5	79.3	78.0	84.6	97
		^{19}F	87.6	29.5	39.2	84.7	28.5	37.9	32.5	
10	0.7717	^{31}P	378.1	363.4	410.4	372.5	357.1	413.7	375	87
		^{17}O	−24.6	−9.7	−2.2	−25.1	−10.0	−2.0		
		^{1}H$_{anti}$	−2.6	−0.7	−1.5	−2.4	−0.7	−1.5		
		^{1}H$_{syn1}$	14.4	10.2	15.0	14.9	10.4	15.6		
		^{1}H$_{syn2}$	−1.9	−0.2	−0.5	−1.4	0.0	−0.1		
11	0.7570	^{31}P	1107.5	1040.0	1002.6	1151.2	1083.4	1044.3	1030.8	91
		^{19}F$_{ax}$	260.0	194.2	206.4	261.2	194.7	206.1	226.8	
		^{19}F$_{eq}$	33.3	19.9	32.0	32.2	19.5	32.1	35	
		^{1}H	17.8	15.8	24.6	17.6	15.6	25.1	38.5	
12	0.8065	^{31}P	−122.2	−39.8	−20.9	−127.7	−42.0	−18.3	−29	116
		^{17}O	−21.0	−8.4	−7.4	−21.9	−9.0	−8.2		
		^{17}O(H)	2.0	0.6	0.9	1.8	0.6	0.9		
		^{1}H	−0.4	−0.1	−0.7	−0.2	0.0	−0.6		
13	0.7661	^{31}P	160.4	57.1	45.5	160.9	57.3	35.4	68	89
		^{35}Cl	6.3	2.2	3.2	6.4	2.2	3.0	0.6	
14	0.7588	^{31}P	1347.0	1271.9	1275.0	1404.2	1330.4	1341.7	1330	91
		^{19}F$_{ax}$	303.4	235.9	255.7	302.2	234.7	252.6	291	
		^{19}F$_{eq}$	43.3	33.7	50.9	39.8	31.5	48.8	60	
15	0.8147	^{31}P	−147.7	−48.5	−19.9	−147.5	−47.3	−20.8	−44.3	86
		^{35}Cl	−1.6	−0.5	−0.9	−1.8	−0.7	−1.2	−4.5	
		^{17}O	−16.3	−6.0	−5.4	−18.2	−7.6	−6.0		
16	0.7861	^{31}P	1217.2	1140.3	1250.1	1283.8	1198.1	1317.9	1233	96
		^{35}Cl$_{ax}$	23.9	20.9	27.5	28.5	24.5	30.7	35	
		^{35}Cl$_{eq}$	0.0	0.7	1.5	−0.1	0.9	2.0		
17	0.7571	^{31}P	−49.1	−16.2	−37.0	−52.0	−17.2	−38.2	−39.1	85
		^{19}F	−12.4	−3.7	−9.7	−11.9	−3.5	−9.1	−8	
		^{17}O$_{ax}$	−3.4	−1.6	−2.1	−3.3	−1.5	−2.1		
		^{17}O$_{eq}$	−29.0	−9.8	−15.5	−29.1	−9.8	−15.5		
18	0.7560	^{31}P	1378.7	1298.6	1281.1	1464.7	1384.4	1364.7	1328.2	88
		^{19}F$_{ax}$	−6.4	−1.7	0.2	−8.0	−2.1	0.3		
		^{19}F$_{eq}$	208.3	159.7	183.9	202.5	154.1	175.5	206.6	
19	0.7865	^{31}P	1453.0	1311.7	1332.7	1685.7	1500.7	1537.8	1371	96
		^{35}Cl$_{ax}$	39.0	29.6	33.7	34.2	26.2	31.9	40	
		^{35}Cl$_{eq}$	11.3	10.1	15.5	45.0	34.6	38.3	20	
		^{17}O	2.2	−0.5	−1.4	6.0	0.6	−2.7		
20	0.7791	^{31}P	1182.0	1097.1	1123.5	1212.0	1124.2	1161.1		
		^{35}Cl	36.2	27.7	32.4	37.9	29.2	33.7		
		^{33}S	−3.0	0.3	2.1	−2.6	0.7	1.4		
		^{19}F	−2.7	6.5	15.9	−4.6	5.1	15.6		
21	0.7813	^{31}P	1655.3	1539.8	1586.0	1699.1	1577.9	1642.2	1617	96
		^{35}Cl$_{ax}$	−3.1	−0.9	−1.3	−3.0	−0.9	−1.0		
		^{35}Cl$_{eq}$	12.9	10.7	12.9	13.6	11.3	13.2	23.3	
22	0.7942	^{31}P	−77.6	−25.2	−12.7	−82.9	−26.9	−8.6	−19.2	99
		^{17}O$_{ax}$	1.1	0.4	−0.2	1.2	0.4	−0.2		
		^{17}O$_{eq}$	−31.0	−14.2	−11.4	−31.4	−14.7	−12.5		
23	0.7766	^{31}P	−26.0	−8.4	−19.0	−25.3	−8.2	−18.1	−16.8	98
		^{33}S	18.7	10.9	12.4	19.0	11.2	11.8		
		^{17}O	1.2	0.4	0.5	1.1	0.4	0.5		
24	0.7606	^{31}P	−13.0	−5.2	−15.5	−14.5	−5.7	−17.0	−13.5	98
		^{33}S$_{ax}$	2.6	1.4	2.3	3.2	1.8	2.8		
		^{33}S$_{eq}$	11.1	4.1	9.3	11.9	4.3	8.2		
		^{17}O	1.3	0.3	0.6	1.2	0.3	0.6		
25	0.7780	^{31}P	−24.7	−8.0	−21.3	−24.5	−8.1	−21.7	−14.7	98
		^{33}S$_{ax}$	−0.4	−0.1	−0.3	−0.4	−0.1	−0.3		
		^{33}S$_{eq}$	16.7	9.4	10.8	17.0	9.6	10.0		

[a] Calculated using the 6-311G** basis set. [b] Hyperfine couplings are usually reported as absolute values; negative signs have been assumed in certain instances (in agreement with all levels of theory). [c] Additional experimental references are detailed in the text for many cases.

TABLE 3: Calculated and Experimental Hyperfine Couplings for Radicals 17–25 with Diffuse Functions Added to the Basis Set[a]

radical	HF $\langle S^2 \rangle$	nucleus	isotropic hyperfine coupling, G						expt[b]	ref[c]
			UHF/6-31G** geometry			MP2/6-31G** geometry				
			UHF	PUHF	UMP2	UHF	PUHF	UMP2		
17	0.7584	^{31}P	-50.3	-16.5	-37.7	-53.5	-17.6	-38.9	-39.1	85
		^{19}F	-12.6	-3.7	-9.6	-12.2	-3.6	-9.0	-8	
		^{17}O$_{ax}$	-3.9	-1.8	-2.5	-3.7	-1.6	-2.4		
		^{17}O$_{eq}$	-30.1	-10.1	-16.8	-30.1	-10.1	-16.8		
18	0.7559	^{31}P	1313.6	1239.9	1233.6	1404.9	1331.0	1324.7	1328.2	88
		^{19}F$_{ax}$	-6.0	-1.4	1.8	-7.9	-2.2	1.8		
		^{19}F$_{eq}$	197.7	153.5	177.0	193.1	147.9	169.2	206.6	
19	0.7874	^{31}P	1437.0	1294.1	1322.6	1672.3	1482.9	1533.5	1371	96
		^{35}Cl$_{ax}$	39.5	29.7	34.0	34.5	26.2	31.9	40	
		^{35}Cl$_{eq}$	11.5	10.0	15.4	45.4	34.6	38.7	20	
		^{17}O	1.9	-0.8	-2.0	5.7	0.5	-3.5		
20	0.7797	^{31}P	1174.5	1089.1	1118.4	1203.9	1115.6	1156.3		
		^{35}Cl	36.7	27.9	33.0	38.4	29.3	34.2		
		^{33}S	-2.3	0.8	1.8	-1.9	1.1	2.1		
		^{19}F	-2.2	8.4	19.5	-4.0	7.0	19.5		
21	0.7820	^{31}P	1645.9	1530.5	1581.3	1687.2	1577.9	1635.9	1617	96
		^{35}Cl$_{ax}$	-2.9	-0.9	-1.1	-2.7	-0.9	-0.8		
		^{35}Cl$_{eq}$	13.6	11.0	13.1	14.3	11.3	13.4	23.3	
22	0.8125	^{31}P	-78.3	-25.5	-15.0	-83.4	-27.0	-11.6	-19.2	99
		^{17}O$_{ax}$	0.8	0.3	-0.4	1.0	0.4	-0.4		
		^{17}O$_{eq}$	-34.8	-15.5	-11.5	-35.3	-16.0	-12.3		
23	0.7803	^{31}P	-25.7	-8.2	-18.4	-26.0	-8.4	-19.0	-16.8	98
		^{33}S	18.5	10.9	13.0	18.8	11.2	12.3		
		^{17}O	1.1	0.4	0.5	1.1	0.4	0.5		
24	0.7615	^{31}P	-13.5	-5.0	-16.4	-15.1	-5.5	-17.9	-13.5	98
		^{33}S$_{ax}$	2.7	1.4	2.6	3.3	1.8	3.0		
		^{33}S$_{eq}$	10.9	4.1	9.5	11.6	4.3	8.3		
		^{17}O	1.3	0.4	0.5	1.2	0.3	0.5		
25	0.7798	^{31}P	-24.7	-8.0	-21.3	-24.8	-8.0	-21.2	-14.7	98
		^{33}S$_{ax}$	-0.4	-0.1	-0.3	-0.4	-0.1	-0.3		
		^{33}S$_{eq}$	16.1	9.5	11.5	17.0	9.8	10.7		

[a] Calculated using the 6-311+G* basis set (protons do not appear in any of these radicals). [b] Hyperfine couplings are usually reported as absolute values; negative signs have been assumed in certain instances (in agreement with all levels of theory). [c] Additional experimental results are detailed in the text for many cases.

of the molecules exhibiting HF doublet instability in this study. While experimental data are not available for **8**, the MP2 predicted ^{31}P hfs is in accord with other dioxophosphoranyl analogs (vide infra). Nevertheless, it seems likely that a multiconfigurational treatment is warranted should more quantitative accuracy be required.

PF$_2$($^2B_1$). Nelson et al.[97] have observed **9** in a xenon matrix at both 77 and 4.2 K; the radicals are freely tumbling at the former temperature and rigid at the latter. Measured isotropic hfs values are in good accord with PUHF and MP2 predictions. The UHF level, on the other hand, does very poorly in this regard.

Me$_2$PO($^2A'$). Compared to **5**, the predicted geometry of **10** shows less sensitivity to level of theory, although the P–O bond distance still lengthens by a sizable 0.026 Å upon inclusion of correlation at the MP2 level. This change in bond length does not appear to affect the predicted hyperfine couplings at any level, however. All levels are in reasonable agreement with an experimental measurement at 77 K in Me$_3$PO powder.[87] Tordo and co-workers succeeded in measuring an ^{17}O hfs of –9.3 G in the analogous phosphonyl radical substituted at phosphorus with two 2,4,6-tri-*tert*-butylphenyl groups.[114,115] However, the extremely bulky nature of these groups makes it unclear how relevant this value is to **10**. It is noteworthy that the predicted ESR data for **5** are reasonably close to those for **10** at their respective UMP2 geometries but differ significantly at the UHF geometries, suggesting that in the former instance one really cannot afford to ignore correlation.[112]

HPF$_3$($^2A'$). Radical **11** is another member of the fluorophosphoranyl series which has seen extensive experimental[19,91,92,97] and theoretical[3,19,34] study. We have discussed the fluorophosphoranyl series in more detail elsewhere[34] and point out here only the good agreement between experimental and MP2-derived hfs values for all four distinct nuclei.

PO$_2$(OH)$_2$($^2B_1$). X-irradiation of KH$_2$PO$_4$, KD$_2$PO$_4$, and Ca(H$_2$PO$_4$)$_2$ has been performed at 77 K to generate radical

12.[98,116] The MP2 predicted hyperfine couplings are in good agreement with experiment. The UHF predictions are quite far off, no doubt due in part to fairly high spin contamination and to HF doublet instability, which manifests in an unusually strong predicted IR absorption at 2443 cm^{-1}.

PCl$_2$($^2B_1$). Radical **13** has been observed in PCl$_3$ matrices at liquid nitrogen temperatures and below.[89,93] The calculated hfs values show a sensitivity to levels of theory and geometry quite similar to **9**. Aagaard et al.[17] have previously calculated the structure of PCl$_2$ at the ROHF/3-21G$^{(*)}$ level, obtaining a bond length of 2.038 Å and a bond angle of 101.9°, in surprisingly close agreement with the present higher level calculations. Their study did not calculate predicted hfs values for **13**, however.

PF$_4$($^2A_1$). Perfluorophosphoranyl has seen considerable experimental study under a variety of conditions.[19,91,92,97,117] A complete discussion of the various theoretical treatments is provided elsewhere.[34] As with the other members of the fluorophosphoranyl series, the predicted isotropic hyperfine couplings for **14** are in reasonably good agreement with experiment.

PCl$_2$O$_2$($^2B_2$). Radical **15**, like the other dioxophosphoranyls, suffers from HF doublet instability as evidenced by a tendency to break the symmetry of the electronic wave function if allowed and an unusually strong predicted IR absorption at 2095 cm^{-1}. This instability probably contributes to the large 5.3° change in the OPO bond angle on going from the UHF geometry to the UMP2. However, this change does not appear to have much effect on the calculated hfs values, which in this instance agree best with the experimental[86] ^{31}P measurement for the PUHF derived splittings. In this case the experimental measurement was taken in a POCl$_3$ matrix at 77 K.

PCl$_4$($^2A_1$). Radical **16** is distorted from the more typical TBP$_e$ geometry observed for its fluorine analog **14** by having a bond angle 18° smaller between the two "axial" chlorine atoms. This is again in remarkably good agreement with earlier calculations

TABLE 4: Error Analysis for Prediction of Isotropic Hyperfine Couplings[a,b]

computational method				error analysis				regression analysis			
subset	geom[c]	+?[d]	$P^{\alpha-\beta}_{\mu\nu}$	mean error, G	stand dev, G	unsigned error, G	rms error, G	corr const R^2	slope	int, G	std error, G
all	UHF	no	UHF	6.9	45.6	31.0	45.6	0.9928	0.959	6.22	41.3
all	UHF	no	PUHF	−20.1	27.3	24.0	33.6	0.9979	1.036	9.7	22.1
all	**UHF**	**no**	**MP2**	**−10.5**	**20.7**	**16.5**	**22.9**	**0.9986**	**1.022**	**3.9**	**18.2**
all	MP2	no	UHF	20.7	72.3	45.6	74.3	0.9889	0.902	11.8	51.0
all	MP2	no	PUHF	−7.7	34.7	24.8	35.1	0.9953	0.978	14.4	33.4
all	MP2	no	MP2	2.5	36.5	21.1	36.1	0.9959	0.960	10.0	30.9
anions[e]	UHF	no	UHF	4.7	34.6	21.9	33.6	0.9992	0.955	11.2	18.2
anions	UHF	no	PUHF	−15.5	29.7	23.3	32.4	0.9993	1.040	2.2	17.6
anions	**UHF**	**no**	**MP2**	**−12.6**	**16.7**	**14.0**	**20.4**	**0.9999**	**1.024**	**4.5**	**7.8**
anions	UHF	yes	UHF	−3.2	27.9	17.8	27.0	0.9989	0.972	12.8	22.1
anions	UHF	yes	PUHF	−22.5	39.3	30.3	44.0	0.9994	1.061	3.0	16.6
anions	UHF	yes	MP2	−18.2	28.0	19.0	32.4	0.9993	1.037	5.9	17.0
anions	MP2	no	UHF	33.8	97.8	52.1	99.8	0.9934	0.883	10.7	53.6
anions	MP2	no	PUHF	9.6	45.0	28.8	44.3	0.9959	0.969	1.5	42.0
anions	MP2	no	MP2	15.1	48.7	24.7	49.2	0.9970	0.948	3.5	36.2
anions	MP2	yes	UHF	26.3	90.4	46.6	90.8	0.9926	0.896	12.2	56.5
anions	MP2	yes	PUHF	3.6	39.4	23.8	38.0	0.9964	0.983	2.3	39.6
anions	MP2	yes	MP2	10.4	47.8	21.6	47.1	0.9962	0.957	4.9	40.4
uncharged[f]	UHF	no	UHF	8.1	51.5	35.1	51.1	0.9856	0.959	3.6	49.7
uncharged	UHF	no	PUHF	−20.6	26.4	23.0	33.1	0.9965	1.028	13.5	24.6
uncharged	**UHF**	**no**	**MP2**	**−7.5**	**20.3**	**16.2**	**21.3**	**0.9977**	**1.014**	**3.8**	**20.0**
uncharged	MP2	no	UHF	15.4	58.9	43.1	59.7	0.9862	0.921	7.9	48.7
uncharged	MP2	no	PUHF	−13.6	24.9	21.3	27.9	0.9964	0.986	17.4	24.7
uncharged	MP2	no	MP2	−0.4	25.9	18.2	25.4	0.9971	0.967	9.6	22.5
all/P hfs[g]	UHF	no	UHF	13.4	61.9	49.0	61.8	0.9911	0.956	10.5	57.3
all/P hfs	UHF	no	PUHF	−20.2	32.8	26.5	37.8	0.9986	1.043	−1.9	22.7
all/P hfs	**UHF**	**no**	**MP2**	**−10.0**	**27.0**	**20.8**	**28.2**	**0.9986**	**1.027**	**−4.3**	**22.6**
all/P hfs	MP2	no	UHF	39.6	97.8	76.3	103.1	0.9862	0.895	20.8	71.5
all/P hfs	MP2	no	PUHF	3.5	41.4	27.5	40.5	0.9955	0.981	6.9	40.8
all/P hfs	MP2	no	MP2	15.1	46.9	29.2	48.2	0.9954	0.960	6.9	41.1
all/F hfs[h]	UHF	no	UHF	12.9	23.4	18.6	25.4	0.9745	0.937	−2.8	23.3
all/F hfs	UHF	no	PUHF	−30.0	24.8	31.1	37.9	0.9952	1.205	5.6	10.2
all/F hfs	**UHF**	**no**	**MP2**	**−15.4**	**16.3**	**17.1**	**21.7**	**0.9986**	**1.129**	**−1.8**	**5.4**
all/F hfs	MP2	no	UHF	12.8	25.2	20.5	26.8	0.9732	0.918	0.5	23.9
all/F hfs	MP2	no	PUHF	−30.1	23.8	31.2	37.4	0.9929	1.184	8.3	12.3
all/F hfs	MP2	no	MP2	−16.2	16.1	17.6	22.1	0.9970	1.119	0.5	8.0
all/Cl hfs[i]	UHF	no	UHF	−5.9	8.6	8.3	9.9	0.7248	1.026	5.5	9.5
all/Cl hfs	UHF	no	PUHF	−8.6	8.4	10.2	11.6	0.7930	1.355	4.7	8.2
all/Cl hfs	**UHF**	**no**	**MP2**	**−5.5**	**7.0**	**7.3**	**8.5**	**0.8435**	**1.195**	**2.8**	**7.1**
all/Cl hfs	MP2	no	UHF	−1.0	14.0	10.6	13.0	0.4356	0.623	8.0	13.5
all/Cl hfs	MP2	no	PUHF	−5.1	12.0	10.8	12.2	0.4876	0.833	7.5	12.9
all/Cl hfs	MP2	no	MP2	−2.1	11.4	9.0	10.8	0.5655	0.780	6.0	11.9
all/H hfs[j]	UHF	no	UHF	−11.2	6.2	11.2	12.5	0.9974	0.957	13.7	5.4
all/H hfs	UHF	no	PUHF	−19.6	23.0	22.3	28.4	0.9924	1.307	4.2	9.2
all/H hfs	**UHF**	**no**	**MP2**	**−11.4**	**7.9**	**11.4**	**13.4**	**0.9986**	**1.084**	**6.5**	**3.9**
all/H hfs	MP2	no	UHF	−12.0	5.3	12.0	12.9	0.9977	0.968	13.8	5.1
all/H hfs	MP2	no	PUHF	−20.2	23.7	23.0	29.3	0.9922	1.321	4.3	9.3
all/H hfs	MP2	no	MP2	−11.5	8.5	11.5	13.8	0.9984	1.091	6.1	4.3

[a] All errors are relative to experimental data; the best method within a given set appears in boldface. [b] Data are from Tables 2 and 3. [c] Using 6-31G** basis set. [d] Refers to whether diffuse functions were added to the 6-311G** basis set. [e] Compounds 17–25. [f] Compounds 4–16. [g] Twenty data points. [h] Eight data points. [i] Seven data points. [j] Five data points.

by Aagaard et al. at the ROHF/3-21G(*) level.[17] Interestingly, this movement toward more of a distorted tetrahedral (DT) structure does not change the predicted ^{31}P hyperfine couplings much by comparison to **14**. This appears to be the case experimentally as well, although there is some sensitivity of the hyperfine couplings to the composition of the host matrix.[17,86,96]

FPO₃⁻(²A″). Radical **17** is one of the few polyoxophosphoranyls in this study which does *not* appear to suffer from HF doublet instability. However, there is still a large variation in predicted hfs values with respect to level of theory. Although there is very little spin contamination, the MP2 values provide a considerably improved agreement with experiment[85] compared to UHF and PUHF. The experimental measurement refers to irradiated KPO₂F₂ at 77 K.

PF₅⁻(²A₁). The unpaired spin density in **18** resides primarily on the central phosphorus and the four equatorial fluorine atoms. This observation agrees well with earlier calculations at the UHF/4-31G level by Janssen et al.[39] At all levels of theory, the

agreement with experimental measurements[88,118,119] is reasonably good, in part because of the very low spin contamination observed for **18**.

POCl₃⁻(²A′). Radical **19** undergoes a 26° compression of the Cl–P–Cl bond angle and a 0.2-Å lengthening of the unique P–Cl bond on going from the UHF to the UMP2 geometry! While this does not much affect the predicted hfs values for the equivalent chlorine atoms, it has a sizable effect on the remaining atoms, and predictions at the UHF geometry appear to correlate much more closely with experiment.[36,86,96] It seems likely that higher levels of theory will be required to converge the geometry, but they are outside the scope of this present effort.

FPCl₂S⁻(²A′). Like **16** and **19**, **20** is at least as DT-like in geometry as it is TBP_e. Experimentally, it is not possible to resolve the full hyperfine tensor for this radical, although the resolved components are in reasonable accord with the predicted values.[24] Our present calculated structures are in good agreement with the earlier UHF/4-31G structure of Janssen and Buck.[24] These
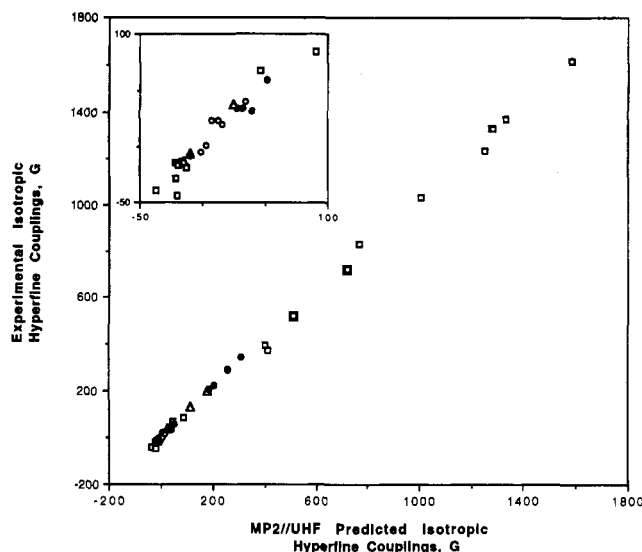
Figure 2. Linear regression representing the third row in Table 4. Open circles refer to ^{35}Cl, open squares to ^{31}P, open triangles to ^{19}F, and filled circles to ^1H. The inset expands the region from –50 to 100 G.

authors discuss the substitution pattern in **20** with respect to traditional notions of apicophilicity. Although from a geometric standpoint it is perhaps not clear to what extent two chlorine atoms separated by a bond angle of only 130° can truly be thought of as apical, it is noteworthy that the ^{35}Cl hyperfine couplings are consistent with the large values typically observed for axially substituted "true" TBP_e compounds, just as the small ^{19}F coupling is consistent with equatorial substitution in such species.

$PCl_5^-(^2A_1)$. The unpaired spin density in **21** resides primarily on the central phosphorus and the four equatorial chlorine atoms. This observation agrees well with the fluorinated analog **18** and earlier calculations at the ROHF/3-21G(*) level by Aagaard et al.[17] At all levels of theory, the agreement with experimental measurements[96] is reasonable, keeping in mind that accurate ^{35}Cl hyperfine couplings are more challenging to obtain experimentally (vide infra).

$PO_4^{2-}(^2B_2)$. Predisposition to break the symmetry of the electronic wave function and an anomalistically intense predicted IR absorption at 2093 cm^{-1} identify **22** as suffering from HF doublet instability. As in earlier instances, the UHF predicted hyperfine splittings are in much poorer agreement with experiment[95,99] than are the other two methods. Surprisingly, neither for **22** nor for any of the other dianions do diffuse functions appear to have much effect on the predicted hfs values.

$PO_2S_2^{2-}(^2B_2)$. HF doublet instability in **23** is easily identified by the predicted imaginary IR frequency. Once again, however, the MP2 predicted ^{31}P hfs couplings are in close agreement with experiment.[98]

$POS_3^{2-}(^2A'')$. Radical **24** exhibits all of the same characteristics as **23** except that the molecular point group is necessarily of lower symmetry. Comparison to the experimental[98] ^{31}P isotropic hfs is again excellent using the MP2 densities.

$PS_4^{2-}(^2B_2)$. Like **22**, **25** undergoes Jahn–Teller distortion to a C_{2v} structure, and like **23** and **24**, it has an imaginary frequency arising from HF doublet instability. Similarly, the experimentally observed[98] isotropic ^{31}P hfs is bracketed by the predicted PUHF and UMP2 values and slightly further from the predicted UHF values.

Error and Regression Analyses

A few caveats should be borne in mind when considering the analyses presented in Table 4. First, the magnitudes of the various error analysis terms are strongly dependent on the nature of the data set. In particular, the magnitudes of the unsigned errors for the sets containing only one type of atom, regardless of level of theory, reflect both the size of the atomic magnetogyric ratio and the tendency for individual atoms to accept spin density. Put

more concretely, the error is largest for phosphorus because the data set for phosphorus spans a much larger range of hfs values than for any other element. Although in principle the data could be made more uniform by putting everything on a percentage basis, this leads to difficulties with the many coupling constants near zero. In sum, the error analyses are useful for identifying qualitative relationships between parameters being varied, but should not be viewed too literally.

The regression analyses, on the other hand, say more about the consistency of predicted hyperfine couplings than about their accuracy. Obviously, the ideal methodology would deliver a regression with a linear slope of unity, a zero intercept, a zero standard error, and a correlation constant of unity. These two different approaches to assessing various methodologies provide complementary perspectives for comparison purposes.

Table 4 is divided into seven distinct subsections, one treating the entire set of 40 data points, one each for the data from anions and uncharged molecules treated separately (there are insufficient cations for a statistically useful treatment), and one section for each of the four atoms taken separately. Within each section, the combination of variables which gave the lowest standard error in the linear regression is in boldface; in every instance that is the MP2/6-311G** derived hfs values calculated at the HF/6-31G** optimized geometries (hereafter referred to a MP2//UHF). This combination also gave the best correlation coefficient and the lowest overall rms and unsigned error in six of the seven cases. In the proton only data set, the rms and unsigned error for the UHF predicted hfs values were very slightly lower than for the MP2; although since there are only five data points, this is not particularly meaningful. The PUHF//UHF hyperfine splittings are less good in quality, but since these values do not require calculation of the MP2 spin density matrix, the considerably greater speed of this method makes it a potentially attractive alternative for very large radicals.

It is noteworthy that, within the set of anions, there is no improvement in predictive abilities upon inclusion of diffuse functions on the heavy atoms (there are no protons) in **17–25**. Indeed, Tables 2 and 3 indicate that there is very little change in any of the predicted hyperfine splittings except for radical **18**, where the ^{31}P hfs value is predicted to be 40–60 G lower when diffuse functions are included. This lower prediction decreases the correlation for the MP2//UHF predictions; however, it would not be reasonable based on **18** alone to suggest that diffuse functions should be expected to decrease predictive capability in general. Rather, it is clear that at least within this set of compounds, they offer no general *increase* in predictive accuracy. Although diffuse functions are well known to be required for accurate molecular energies in negatively charged systems, these calculations appear to indicate that the spin density *at the nuclei* is not changed as a result of permitting the electron density to become more diffuse.

It is interesting to note that the MP2//UHF linear regressions for the full data set, the anions, and the uncharged radicals all provide a best fit slope of about 1.02 with a fairly small intercept. In other words, the MP2//UHF predicted hyperfine couplings may be scaled by 102% to improve agreement with experiment (and, of course, further improvement may be had by adding the intercept). This is not the case, however, in the single-atom data sets. Instead, the excellent correlations obtained for ^{31}P, ^{19}F, and ^1H suggest scaling factors of 103%, 113%, and 108%, respectively. Certainly there is no reason to expect these scaling factors *not* to be different, given that basis function exponents are unique to specific atoms, these three atoms each occupy different rows of the periodic table, etc. However, the number of data available for these individual atom regressions is insufficient to place too much trust in these scaling factors being entirely general; more work remains to be done to establish that. As for ^{35}Cl, interaction of the unpaired electron with the large nuclear quadrupole makes accurate determination of hyperfine splittings more difficult for this nucleus than the others,[24] and this is probably in part

responsible for the very poor correlation between theory and experiment (R^2 = 0.8435 for MP2//UHF) for this particular data set.

One observation that does appear to be quite general is that scaling factors for the MP2//UHF level will be uniformly positive. Indeed, using UHF geometries, the PUHF and MP2 hfs *mean* errors are uniformly negative and the regression slopes are greater than unity in every instance. At the MP2 geometries, this is not the case. This is reminiscent of the situation with respect to prediction of infrared frequencies at the HF and MP2 levels. (Note that this property requires the geometry to be optimized at the same level as the frequency calculation itself, however.) For IR calculations, it is well established that HF stretching frequencies are consistently overestimated by about 10%[58] while MP2 frequencies tend to be more accurate in an absolute sense but less reliable in terms of being subject to some consistent scaling which will bring them into closer agreement with experiment.

It is worth emphasizing, however, that regression analysis is most successful when used in an interpolative sense; i.e., we would expect our scaling prescriptions to be most effective for additional phosphoranyl radicals that closely resemble those discussed here. Extrapolation might be considerably less successful, however, and the practice should never be accepted carelessly. One potentially dangerous example would be the prediction of hyperfine couplings for molecules like Me_3PS^-,[27] Me_3PSEt,[29] and chlorophosphoranyls,[16] all of which have been assigned to have the unpaired electron localized in a P–X antibonding orbital (sometimes called an asymmetric three-electron bond), making them distinct from any system included here. We have examined the H_3PS^- radical anion elsewhere[35] and found it to have a simple TBP_e structure, suggesting that the experimental observations may include subtle dynamic, substituent, and/or condensed-phase effects; more rigorous studies will be required to resolve these issues.

In conclusion, for this data set of 25 reasonably diverse phosphorus-containing radicals from which 40 experimental hyperfine couplings are available for four different nuclei, the most accurate theoretical predictions are obtained from calculations at the MP2/6-311G**//UHF/6-31G** level. Projecting the largest component of spin contamination from the UHF spin-density matrix provides predicted values of lower quality but is also quite a bit less computationally intensive. Diffuse functions do not improve the quality of the hfs predictions for the nine anions and dianions examined here.

Although it is a given that accurate prediction of hyperfine couplings in small molecules should include much higher treatments of electron correlation, as well as an analysis of dynamic effects, this is similar to suggesting that accurate prediction of vibrational frequencies should include high-level treatments of correlation and corrections for anharmonicity. However, such approaches are not yet feasible for larger molecules; instead, it appears that calculation of isotropic hyperfine couplings using the present methodology will serve about as useful a purpose as calculating scaled HF vibrational frequencies using the rigid-rotor harmonic oscillator approximation. By taking advantage of opposing errors implicit in various approximations and correcting for any remaining systematic deviations, useful results may be obtained for comparison with experiment. Interesting future directions would include similar evaluations of ROHF and density functional methods.

Supplementary Material Available: Gaussian92 archive files for MP2/6-31G** optimized geometries of **1–25** (5 pages). Ordering information is given on any current masthead page.

References and Notes

(1) Bentrude, W. G. *Acc. Chem. Res.* **1982**, *15*, 117.

(2) Demolliens, A.; Eisenstein, O.; Hiberty, P. C.; Lefour, J. M.; Ohanessian, G.; Shaik, S. S.; Volatron, F. *J. Am. Chem. Soc.* **1989**, *111*, 5623.

(3) Howell, J. M.; Olsen, J. F. *J. Am. Chem. Soc.* **1976**, *98*, 7119.

(4) Janssen, R. A. J.; Visser, G. J.; Buck, H. M. *J. Am. Chem. Soc.* **1984**, *106*, 3429.

(5) Roberts, B. P. *Tetrahedron Lett.* **1983**, *24*, 3377.

(6) Davies, A. G.; Griller, D.; Roberts, B. P. *J. Chem. Soc., Perkin Trans. 2* **1972**, 993.

(7) Giles, J. R. M.; Roberts, B. P. *J. Chem. Soc., Perkin Trans. 2* **1981**, 1211.

(8) Nakanishi, A.; Nishikida, K.; Bentrude, W. G. *J. Am. Chem. Soc.* **1978**, *100*, 6403.

(9) Nakanishi, A.; Nishikida, K.; Bentrude, W. G. *J. Am. Chem. Soc.* **1978**, *100*, 6398.

(10) Watts, G. B.; Griller, D.; Ingold, K. U. *J. Am. Chem. Soc.* **1972**, *94*, 8784.

(11) Cramer, C. J. *J. Am. Chem. Soc.* **1990**, *112*, 7965.

(12) Cramer, C. J.; Gustafson, S. M. *J. Am. Chem. Soc.* **1993**, *115*, 9315.

(13) Cramer, C. J.; Gustafson, S. M. *J. Am. Chem. Soc.* **1994**, *116*, 723.

(14) Aagaard, O. M.; Janssen, R. A. J.; Buck, H. M. *Recl. Trav. Chim. Pays-Bas* **1989**, *108*, 262.

(15) Aagaard, O. M.; Janssen, R. A. J.; Waal, B. F. M. D.; Buck, H. M. *J. Am. Chem. Soc.* **1990**, *112*, 938.

(16) Aagaard, O. M. Ph.D. Thesis, Technische Universiteit Eindhoven, 1991.

(17) Aagaard, O. M.; Waal, B. F. M. D.; Cabbolet, M. J. T. F.; Janssen, R. A. J. *J. Phys. Chem.* **1992**, *96*, 614.

(18) Berclaz, T.; Geoffroy, M.; Lucken, E. A. C. *Chem. Phys. Lett.* **1975**, *36*, 677.

(19) Colussi, A. J.; Morton, J. R.; Preston, K. F. *J. Phys. Chem.* **1975**, *79*, 1855.

(20) Geoffroy, M.; Rao, G.; Tancic, Z.; Bernardinelli, G. *J. Am. Chem. Soc.* **1990**, *112*, 2826.

(21) Geoffroy, M.; Jouaiti, A.; Terron, G.; Cattani-Lorente, M.; Ellinger, Y. *J. Phys. Chem.* **1992**, *96*, 8241.

(22) Hamerlinck, J. H. H.; Schipper, P.; Buck, H. M. *J. Am. Chem. Soc.* **1980**, *102*, 5679.

(23) Hamerlinck, J. H. H.; Schipper, P.; Buck, H. M. *J. Am. Chem. Soc.* **1983**, *105*, 385.

(24) Janssen, R. A. J.; Buck, H. M. *Chem. Phys. Lett.* **1986**, *132*, 459.

(25) Janssen, R. A. J.; Sonnemans, M. H. W.; Buck, H. M. *J. Chem. Phys.* **1986**, *84*, 3694.

(26) Janssen, R. A. J.; Sonnemans, M. H. W.; Buck, H. M. *J. Am. Chem. Soc.* **1986**, *108*, 6145.

(27) Janssen, R. A. J.; Kingma, J. A. J. M.; Buck, H. M. *J. Am. Chem. Soc.* **1988**, *110*, 3018.

(28) Janssen, R. A. J.; van der Woerd, M. J.; Aagaard, O. M.; Buck, H. M. *J. Am. Chem. Soc.* **1988**, *110*, 6001.

(29) Janssen, R. A. J.; Aagaard, O. M.; van der Woerd, M. J.; Buck, H. M. *Chem. Phys. Lett.* **1990**, *171*, 127.

(30) Kokoszka, G. F.; Brinckman, F. E. *J. Am. Chem. Soc.* **1970**, *92*, 1199.

(31) Krusic, P. J.; Mahler, W.; Kochi, J. K. *J. Am. Chem. Soc.* **1972**, *94*, 6033.

(32) Schipper, P.; Jansen, E. H. J. M.; Buck, H. M. *Top. Phosphorus Chem.* **1977**, *9*, 407.

(33) Symons, M. C. R.; Petersen, R. L. *J. Chem. Soc., Faraday Trans. 2* **1979**, *75*, 210.

(34) Cramer, C. J. *J. Am. Chem. Soc.* **1991**, *113*, 2439.

(35) Cramer, C. J. *Chem. Phys. Lett.* **1993**, *202*, 7034.

(36) Gillbro, T.; Williams, F. *J. Am. Chem. Soc.* **1974**, *96*, 5032.

(37) Gonbeau, D.; Guimon, M.-F.; Ollivier, J.; Pfister-Guillouzo, G. *J. Am. Chem. Soc.* **1986**, *108*, 4760.

(38) Gorlov, Y. I.; Penkovsky, V. V. *Chem. Phys. Lett.* **1975**, *35*, 25.

(39) Janssen, R. A. J.; Buck, H. M. *J. Mol. Struct. (THEOCHEM)* **1984**, *110*, 139.

(40) Barone, V.; Adamo, C.; Russo, N. *Chem. Phys. Lett.* **1993**, *212*, 5.

(41) Carmichael, I. *Chem. Phys.* **1987**, *116*, 351.

(42) Chipman, D. M. *J. Chem. Phys.* **1983**, *78*, 4785.

(43) Cramer, C. J. *J. Mol. Struct. (THEOCHEM)* **1991**, *235*, 243.

(44) Ellinger, Y.; Subra, R.; Berthier, G. *Nouv. J. Chim.* **1983**, *7*, 375.

(45) Feller, D.; Davidson, E. J. *Chem. Phys.* **1983**, *80*, 1006.

(46) Glidewell, C. *Inorg. Chim. Acta* **1984**, *83*, L81.

(47) Knight, L. B.; Earl, E.; Ligon, A. R.; Cobranchi, D. P.; Woodward, J. R.; Bostick, J. M.; Davidson, E. R.; Feller, D. *J. Am. Chem. Soc.* **1986**, *108*, 5065.

(48) Nakatsuji, H.; Izawa, M. *J. Chem. Phys.* **1989**, *91*, 6205.

(49) O'Malley, P. J.; MacFarlane, A. J. *J. Mol. Struct. (THEOCHEM)* **1992**, *277*, 293.

(50) Sekino, H.; Bartlett, R. J. *J. Chem. Phys.* **1985**, *82*, 4225.

(51) Sieiro, C.; de la Vega, J. M. G. *J. Mol. Struct. (THEOCHEM)* **1985**, *120*, 383.

(52) Smith, P.; Donovan, W. H. *J. Mol. Struct. (THEOCHEM)* **1990**, *204*, 21.

(53) Pople, J. A.; Beveridge, D. A. *Approximate Molecular Orbital Theory*; McGraw-Hill: New York, 1970.

(54) Stewart, J. J. P. In *Reviews in Computational Chemistry*; Lipkowitz, K. B., Boyd, D. B., Eds.; VCH: New York, 1989; Vol. 1, p 45.

(55) Zerner, M. C. In *Reviews in Computational Chemistry*; Lipkowitz, K. B., Boyd, D. B., Eds.; VCH: New York, 1990; Vol. 2, p 313.

(56) Knight, L. B.; Arrington, C. A.; Gregory, B. W.; Cobranchi, S. T.; Liang, S.; Paquette, L. *J. Am. Chem. Soc.* **1987**, *109*, 5521.

(57) Dykstra, C. E. *Ab Initio Calculation of the Structures and Properties of Molecules*; Elsevier: New York, 1988; Vol. 58.

(58) Hehre, W. J.; Radom, L.; Schleyer, P. v. R.; Pople, J. A. *Ab Initio Molecular Orbital Theory*; Wiley: New York, 1986.

(59) Szabo, A.; Ostlund, N. S. *Modern Quantum Chemistry*; Macmillan: New York, 1982.

(60) Barone, V.; Minichino, C.; Faucher, H.; Subra, R.; Grand, A. *Chem. Phys. Lett.* **1993**, *205*, 324.

(61) Cramer, C. J. *J. Org. Chem.* **1991**, *56*, 5229.

(62) Lunell, S.; Eriksson, L. A.; Worstbrock, L. *J. Am. Chem. Soc.* **1991**, *113*, 7508.

(63) Knight, L. B.; Steadman, J.; Feller, D.; Davidson, E. *J. Am. Chem. Soc.* **1984**, *106*, 3700.

(64) Knight, L. B.; Earl, E.; Ligon, A. R.; Cobranchi, D. P. *J. Chem. Phys.* **1986**, *85*, 1228.

(65) Knight, L. B.; Winiski, M.; Kudelko, P.; Arrington, C. A. *J. Chem. Phys.* **1989**, *91*, 3368.

(66) Knight, L. B.; Ligon, A.; Cobranchi, S. T.; Cobranchi, D. P.; Earl, E.; Feller, D.; Davidson, E. *J. Chem. Phys.* **1986**, *85*, 5437.

(67) Knight, L. B.; Wise, M. B.; Childers, A. G.; Davidson, E. R.; Daasch, W. R. *J. Chem. Phys.* **1980**, *73*, 4198.

(68) Carmichael, I. *J. Phys. Chem.* **1987**, *91*, 6443.

(69) Barone, V.; Grand, A.; Minichino, C.; Subra, R. *J. Chem. Phys.* **1993**, *99*, 6787.

(70) Barone, V.; Grand, A.; Minichino, C.; Subra, R. *J. Phys. Chem.* **1993**, *97*, 6355.

(71) Buckingham, A. D.; Olegário, R. M. *Chem. Phys. Lett.* **1993**, *212*, 253.

(72) Knight, L. B.; Cobranchi, S. T.; Gregory, B. W.; Earl, E. *J. Chem. Phys.* **1987**, *86*, 3143.

(73) *Density Functional Methods in Chemistry*; Labanowski, J.; Andzelm, J., Eds.; Springer-Verlag: New York, 1991.

(74) Parr, R. G.; Yang, W. *Density-Functional Theory of Atoms and Molecules*; Oxford University Press: New York, 1989.

(75) Ziegler, T. *Chem. Rev.* **1991**, *91*, 651.

(76) Ohta, K.; Nakatsuji, H.; Maeda, I.; Yonezawa, T. *Chem. Phys.* **1982**, *67*, 49.

(77) Chipman, D. M. *Phys. Rev. A* **1989**, *39*, 475.

(78) Edlund, O.; Lund, A.; Shiotani, M.; Sohma, J.; Thuomas, K.-A. *Mol. Phys.* **1976**, *32*, 49.

(79) Poling, S. M.; Davidson, E. R.; Vincow, G. *J. Chem. Phys.* **1971**, *54*, 3005.

(80) Amos, R. T.; Snyder, L. C. *J. Chem. Phys.* **1964**, *41*, 1773.

(81) Claxton, T. A.; Chen, T.; Symons, M. C. R. *Faraday Discuss. Chem. Soc.* **1984**, *78*, 121.

(82) Geoffroy, M.; Terron, G.; Bernardinelli, G. *Chem. Phys. Lett.* **1991**, *182*, 242.

(83) Hameka, H. F. *J. Magn. Reson.* **1987**, *75*, 9.

(84) Atkins, P. W.; Symons, M. C. R. *J. Chem. Soc.* **1964**, 4363.

(85) Begum, A.; Subramanian, S.; Symons, M. C. R. *J. Chem. Soc. A* **1970**, 1323.

(86) Begum, A.; Symons, M. C. R. *J. Chem. Soc. A* **1971**, 2065.

(87) Begum, A.; Symons, M. C. R. *J. Chem. Soc., Faraday Trans. 2* **1973**,m *69*, 43.

(88) Boate, A. R.; Colussi, A. J.; Morton, J. R.; Preston, K. F. *Chem. Phys. Lett.* **1976**, *37*, 135.

(89) Bonazzola, L.; Michaut, J. P.; Roncin, J. *J. Chem. Phys.* **1981**, *75*, 4829.

(90) Brinckman, F. E.; Kokoszka, G. F. *J. Chem. Soc., Chem. Commun.* **1968**, 349.

(91) Colussi, A. J.; Morton, J. R.; Preston, K. F. *J. Chem. Phys.* **1975**, *62*, 2004.

(92) Fessenden, R. W. *J. Magn. Reson.* **1969**, *1*, 277.

(93) Fillam, B. W.; Mishra, S. P.; Symons, M. C. R. *J. Chem. Soc., Dalton Trans.* **1974**, 2145.

(94) Hasegawa, A.; Ohnishi, K.; Sogabe, K.; Miura, M. *Mol. Phys.* **1975**, *30*, 1367.

(95) Hughes, E.; Moulton, W. G. *J. Chem. Phys.* **1963**, *39*, 1359.

(96) Mishra, S. P.; Symons, M. C. R. *J. Chem. Soc., Dalton Trans.* **1976**, 139.

(97) Nelson, W.; Jackel, G.; Gordy, W. *J. Chem. Phys.* **1970**, *52*, 4572.

(98) Picone, R. F.; Raynor, J. B.; Ward, T. C. *J. Chem. Soc., Dalton Trans.* **1977**, 392.

(99) Serway, R. A.; Marshall, S. A. *J. Chem. Phys.* **1966**, *45*, 4098.

(100) Tordo, P. In *Landolt-Börnstein, New Series*; Springer-Verlag: Berlin, 1988; Vol. II, 17/e, p 254.

(101) Frisch, M. J.; Pople, J. A.; Binkley, J. S. *J. Chem. Phys.* **1984**, *80*, 3265.

(102) Krishnan, R.; Binkley, J. S.; Seeger, R.; Pople, J. A. *J. Chem. Phys.* **1980**, *72*, 650.

(103) Schaefer, H. F. *J. Chem. Phys.* **1989**, *91*, 7305.

(104) Benzel, M. A.; Maurice, A. M.; Belford, R. L.; Dykstra, C. E. *J. Am. Chem. Soc.* **1983**, *105*, 3802.

(105) Curtiss, L. A.; Pople, J. A. *Chem. Phys. Lett.* **1987**, *141*, 175.

(106) Kochi, J. K.; Bakuzis, P.; Krusic, P. J. *J. Am. Chem. Soc.* **1973**, *95*, 1516.

(107) Francl, M. M.; Pietro, W. J.; Hehre, W. J.; Bainkley, J. S.; Gordon, M. S.; DeFrees, D. J.; Pople, J. A. *J. Chem. Phys.* **1982**, *76*, 2161.

(108) Chambaud, G.; Levy, B.; Millic, P. *Theor. Chim. Acta* **1978**, *48*, 103.

(109) Cramer, C. J.; Famini, G. R. *J. Am. Chem. Soc.* **1990**, *112*, 5460.

(110) McKelvey, J.; Hehre, W. J. *Mol. Phys.* **1973**, *25*, 983.

(111) Frisch, M. J.; Trucks, G. W.; Head-Gordon, M.; Gill, P. M. W.; Wong, M. W.; Foresman, J. B.; Johnson, B. G.; Schlegel, H. B.; Robb, M. A.; Replogle, E. S.; Gomperts, R.; Andres, J. L.; Raghavachari, K.; Binkley, J. S.; Gonzalez, C.; Martin, R. L.; Fox, D. J.; DeFrees, D. J.; Baker, J.; Stewart, J. J. P.; Pople, J. A. *Gaussian92, Revision D*; Gaussian, Inc.: Pittsburgh, PA, 1992.

(112) Nguyen, M. T.; Ha, T.-K. *Chem. Phys.* **1989**, *131*, 245.

(113) Cramer, C. J.; Famini, G. R. *Chem. Phys. Lett.* **1990**, *169*, 405.

(114) Winter, N. J.; Fossey, J.; Beccard, B.; Berchadsky, Y.; Vila, F.; Werbelow, L.; Tordo, P. *J. Phys. Chem.* **1986**, *90*, 6749.

(115) Ayant, Y.; Thevand, A.; Werbelow, L.; Tordo, P. *J. Magn. Reson.* **1987**, *72*, 251.

(116) McMillan, J. A.; Clemens, J. M. *J. Chem. Phys.* **1978**, *68*, 3627.

(117) Fessenden, R. W.; Schuler, R. H. *J. Chem. Phys.* **1966**, *45*, 1845.

(118) Mishra, S. P.; Symons, M. C. R. *J. Chem. Soc., Chem. Commun.* **1974**, 279.

(119) Morton, J. R.; Preston, K. F.; Strach, S. J. *J. Magn. Reson.* **1980**, *37*, 321.